Food Bioscience 62 (2024) 105141

Contents lists available at ScienceDirect

Food Bioscience

journal homepage: www.elsevier.com/locate/fbio

A soft processing technology for the extraction of cellulose from plant residues and agri-food wastes

Tommaso Bellesia [a], Daniele Carullo [a], Andrea Fachin [a], Enrico Caneva [b], Stefano Farris [a,*]

[a] Department of Food, Environmental and Nutritional Sciences (DeFENS), Food Packaging Laboratory, University of Milan, Milan, Italy
[b] Comprehensive Substances Characterization via Advanced Spectroscopy Technology Platform, University of Milan (UNITECH COSPECT), Milan, Italy

ARTICLE INFO

Keywords:
Biopolymers
Cellulose extraction
Sustainable conversion
Purity
Crystallinity
Surface morphology
Circular economy

ABSTRACT

In this study, cellulose was extracted from giant cane (GC), *Posidonia oceanica* seagrass (PO), coffee silverskin (CS), and brewer's spent grain (BSG) as alternatives to conventional sources of cellulose. The extraction protocol involved three steps: i) hemicellulose and lignin removal through alkaline hydrolysis in a 5% (w/v) NaOH solution (solid-to-liquid ratio = 1:100 g/mL, T = 25 °C, t = 2 h, ω = 300 rpm), ii) removal of organic compounds and ashes through a 95% (v/v) ethanol solution (solid-to-liquid ratio = 1:25 g/mL, T = 25 °C, t = 0.5 h, ω = 500 rpm), and iii) double bleaching in a 1% (w/v) acidic (pH = 4) $NaClO_2$ solution (solid-to-liquid ratio = 1:50 g/mL, T = 90 °C, t = 1.5 h, ω = 500 rpm). Yield, purity, crystallinity degree, and morphology of cellulose extracted through a soft-chemical cascade process were assessed by gravimetric, infrared (FT-IR), nuclear magnetic resonance (NMR) spectroscopy, X-ray diffraction (XRD), and scanning electron microscopy (SEM) analyses. Averaged cellulose extraction yields of 36.4, 38.6, 23.1, and 22.2% for GC, PO, CS, and BSG were obtained, respectively. All cellulose samples had high purity, though lower than the ultra-pure bacterial cellulose, which was due to the slight contamination from unremoved hemicellulose and lignin residues. Cellulose samples exhibited similar chemical features and the typical fibril-like morphology of microcrystalline cellulose (6–13 μm in width). The versatility of the proposed extraction procedure supports the sustainable conversion of low-cost organic biomasses to valuable products with manifold industrial applications (e.g., food packaging).

1. Introduction

In the last decades, the food packaging industry has been striving to replace fossil-based plastics with greener solutions following the sustainability concept, that is, involving eco-friendly processes and raw materials (Asgher et al., 2020; Bangar et al., 2023; El-Sayed & Youssef, 2023; Orqueda et al., 2022). This transition was undoubtedly triggered by the latest legislation (directive EU 2019/904, now under amendment by Regulation EU 2022/0396/COD) demanding the reduction in plastics and their wastes for food packaging applications (Carullo et al., 2023).

Fossil-based plastics, among which polyethylene (PE), polypropylene (PP), polyethylene terephthalate (PET), polystyrene (PS), polyvinyl chloride (PVC), and polyamide (PA), currently dominate the food packaging sector, with a share grazing 40% of the overall plastic market, owing to their cheapness, full recyclability, and superior thermal/mechanical/water vapor barrier performance (Khezerlou et al., 2021; Kumar et al., 2020; Shi et al., 2022). Nevertheless, the underrated environmental burden associated with plastics mismanagement unavoidably generates a huge amount of non-biodegradable waste, thus potentially impairing terrestrial, atmospheric, and marine eco-systems (Beji et al., 2023; Thuy et al., 2021). In an attempt to eliminate or at least minimize this drawback, the development of biodegradable materials for food packaging purposes through the reuse of bio-based sources (e.g., agri-food wastes, but also non-food plant residues) has recently emerged as a pursuable strategy (Apicella et al., 2021; Carullo et al., 2023; Pietrosanto et al., 2022; Pires et al., 2022; Wang et al., 2024). In addition, the utilization of waste for valuable product synthesis has been pointed out as a strategy for mitigating the environmental impact of climate change and managing waste disposal challenges (Iftikhar, Majeed, Altaf, & Khalid, 2024).

Within this scenario, cellulose-based materials are looked at with renewed interest by both academia and industry because of their appealing functional properties, among which high mechanical strength, water absorption capacity, and biodegradability (Huang et al., 2022; Vallejo et al., 2021). Indeed, cellulose is the most abundant organic polymer on earth, which can find valuable application in

* Corresponding author.
E-mail address: stefano.farris@unimi.it (S. Farris).

https://doi.org/10.1016/j.fbio.2024.105141
Received 8 May 2024; Received in revised form 16 September 2024; Accepted 18 September 2024
Available online 18 September 2024

multiple industrial sectors if efficiently recovered from the above-mentioned sources (Khan et al., 2022; Picot-Allain & Emmambux, 2021; Rovera et al., 2023).

In this work, the potential of four different cellulose-rich biomasses, both competing or not with the food sector, for the extraction of cellulose was investigated.

Arundo donax L., commonly referred to as giant cane or giant reed, is a plant species that grows spontaneously in various types of marginal environments, regardless of the type of soil and water availability. Moreover, this infesting plant can be largely found in both temperate and hot regions across the globe (Corno et al., 2014). The stems of giant cane have been recently exploited in disparate sectors, such as building/carpentry, food packaging, and biofuels (Martínez-Sanz et al., 2018).

Posidonia oceanica seagrass is a type of flowering plant that has adapted to life underwater. It preserves Mediterranean ecosystems by preventing coastline erosion and regulating CO_2 absorption in both the sea and the atmosphere (Balata & Tola, 2018). A consistent amount of seagrass residues accumulates on the seashore every year, which often pushes municipalities to remove it through expensive disposal operations due to the negative perceived impact on local tourism. *Posidonia oceanica* biomass, representing a total amount ranging between 5 and 50 Mton per year, is currently dumped into landfills, contributing to raising pollution levels via degradation to smelly compounds (Restaino et al., 2023; Voca et al., 2019). The rapid expansion rates and the lower lignin load as compared to common plants make seagrass a surrogate source for cellulose extraction of conventionally employed biomasses, such as wood and cotton (Tarchoun et al., 2019).

As far as agri-food wastes are concerned, interesting case studies are given by the processing of coffee beans and barley grains for beer-making, whose global production was recently estimated to reach 5.7 Mton and 144.4 Mton, respectively (FAOSTAT, 2022). Harvesting and industrial processing phases generate substantial quantities of biomass wastes from both coffee and barley grains, which stand up to 30%–45% of the total raw materials (Forcina et al., 2023; Mussatto, 2014). These wastes mainly consist of silverskin left after the roasting of coffee beans and the insoluble undegraded part of the barley grain, known as brewer's spent grain (Overturf et al., 2021; Qazanfarzadeh et al., 2023). Interestingly, these wastes are abundant sources of cellulose (≈ 20% dry weight biomass, DW_b), which could be potentially recovered through a biorefinery process and destined for several industries (Iadecola et al., 2022; Liu et al., 2023).

In a previous study, a fast and simple cascade method was developed for the extraction of cellulose from three different feedstocks (i.e., garlic stalks, corncob, and giant cane cut up) for potential usage in the food packaging sector (Rovera et al., 2023). Fourier-Transform Infrared (FT-IR) and Nuclear magnetic resonance (NMR) spectroscopy analyses revealed a relatively high purity degree of the extracted cellulose as compared to cellulose of bacterial origin. This was attributed to the non-negligible presence of traces from other plant components, namely hemicellulose and lignin, following the extraction process. In addition, the values of extraction yields approached the theoretical content of cellulose in biomasses. However, the protocol described by Rovera et al. (2023), while bringing interesting results and time-saving when compared with strong acids/alkali-based cellulose extraction methods (Reddy & Rhim, 2018), still has great room for improvement from an environmental standpoint.

Based on these premises, this study aimed to address some unresolved aspects present in previous works. More specifically, we attempted to improve previous protocols by developing a unique and versatile method that can be universally and interchangeably applied to different agri-food biomasses for cellulose recovery. Our goal was to reduce the overall chemical load by replacing (at least partially) conventional harsh chemicals with safer alternatives. To this end, we decided to use four well-known and widely available lignocellulosic biomasses, namely giant cane, seagrass, coffee silverskin, and brewer's spent grain. The selection of these biomasses was based on their origin: giant cane and seagrass represent natural residues not directly linked to human activity, whereas coffee silverskin and brewer's spent grain are residues from the food industry. This approach aims to demonstrate that the same protocol can be efficiently applied to biomasses with different origins and compositions (Table 1). Moreover, the novelty of this work lies in i) using a lower amount of NaOH for hemicellulose and lignin hydrolysis and ii) replacing the highly toxic xylene with a less-polluting organic solvent (i.e., ethanol) for the removal of the organic compounds. Cellulose extracted from the newly proposed process underwent a systematic characterization in terms of yield, chemical composition/purity, structural organization, and morphology. This work aligns with current research efforts to reduce agricultural waste as a way to mitigate the threats associated with landfilling and GHG emissions (Majeed et al., 2023).

2. Materials and methods

2.1. Raw materials and chemicals

Giant cane (coded as GC) cut-up was obtained in June 2023 from the experimental farm 'A. Menozzi' of the University of Milan (Landriano, Italy). *Posidonia oceanica* seagrass (coded as PO) was manually collected from the Sardinian shore (Alghero, Italy) between May and June 2023. A sample of about 5 kg of seagrass was washed with tap water to remove sand and subsequently stored at 4 °C. Seagrass was transported to the laboratory in an EPS box under refrigerated conditions and delivered within 24 h. Silverskin from *robusta* variety coffee beans (coded as CS) and brewer's spent grain (coded as BSG) were gently provided by the "Caffè Milani" company (Lipomo, Italy) and a craft brewery located in Milan (Italy), respectively, in September 2023. After their arrival at the laboratories, GC, PO, CS, and BSG were separately air-dried at 60 °C (Memmert UF110plus, Schwabach, Germany) and further ground/sieved to yield powders of ≈ 200 μm average size (Rovera et al., 2023). All the pulverized samples were then stored in a desiccator for one week before being processed. Table 1 reports the initial composition of the investigated matrices according to the literature. All chemicals employed in this work, whose material safety data sheets (MSDSs) were reported in Figs. S1–S3 of the Supplementary Material, were of reagent grade (VWR International S.r.l., Milan, Italy) and used without further purification. Grade 230 Whatman filter paper (particle retention: 20–30 μm) for vacuum filtration was acquired from Merck KGaA (Darmstadt, Germany). All solutions were prepared using milli-Q water with a resistivity of 18.2 MΩ cm at 25 °C.

2.2. Cellulose extraction

The recovery of cellulose from the different biomasses was executed

Table 1
Putative composition of the lignocellulosic biomasses tested in this work.

Biomass	Cellulose (%)	Hemicellulose (%)	Lignin (%)	Organic compounds and ashes (%)	Reference
GC	33.7 ± 3.9	24.6 ± 6.3	22.2 ± 2.7	14.2 ± 4.2	Corno et al. (2016)
PO	40.0	18.2	29.1	12.6	Voća et al. (2019)
CS	23.8 ± 0.1	16.7 ± 1.3	28.6 ± 0.5	25.1 ± 3.4	Ballesteros et al. (2014)
BSG	24.0 ± 1.6	9.4 ± 0.7	3.3 ± 0.4	63.0 ± 0.2	Castro and Colpini (2021)

Legend: GC = giant cane, PO = *Posidonia oceanica*, CS = coffee silverskin, BSG = brewer's spent grain.

following the three-step procedure developed by Rovera et al. (2023) but with slight modifications aimed at reducing the environmental footprint of the whole process (Fig. 1). Specifically, 2 g of each powder underwent i) hemicellulose and lignin removal through alkaline hydrolysis in a 5% (w/v) NaOH solution (solid-to-liquid ratio = 1:100 g/mL), ii) further removal of organic compounds and ashes through solvent extraction in a 95% (v/v) ethanol solution (solid-to-liquid ratio = 1:25 g/mL), and iii) ultimate bleaching in a 1% (w/v) $NaClO_2$ solution at pH = 4 (solid-to-liquid ratio = 1:50 g/mL). The last step was repeated twice to ensure full whitening of the final cellulose. After each stage, the separation between the solid and the liquid phases was carried out via Buchner filtration, followed by washing and drying of the residual biomass (Rovera et al., 2023). The processing conditions (SL ratio, time, temperature, and stirring speed) used in this study (Fig. 1) were determined based on preliminary tests, which helped identifying the optimal combination of factors to maximize the extraction yield from all tested biomasses (data not shown). For comparison purposes, ultra-pure bacterial cellulose (BC) was obtained as illustrated in Rovera et al. (2018) and used as a reference substrate.

2.3. Characterization of cellulose samples

2.3.1. Extraction yield

The cellulose extraction yield (Y_C, in %) from all analyzed matrices was gravimetrically estimated as follows (Eq. (1)):

$$Y_C = \frac{m_{CE,i}}{m_{0,i}} \quad (1)$$

where $m_{CE,i}$ is the mass of the dry cellulose extracted from the i-th raw material (i = GC, PO, CS, and BSG) and $m_{0,i}$ represents the mass of the initial biomass (dry powder) used for the extraction (2 g).

2.3.2. Fourier transform infrared spectroscopy (FT-IR)

Attenuated total reflectance infrared (ATR FT-IR) spectra of the extracted cellulose were collected through an IR spectrometer (Spectrum 100, PerkinElmer Inc., USA) utilizing a germanium crystal set at an incident angle of 45°. The spectra were recorded at a 4 cm^{-1} resolution and in the wavenumber range of 4000–800 cm^{-1}. A background spectrum of a clean Ge crystal in air was obtained and used to erase any signal originating from air and moisture. Finally, the baseline modification was applied for the resulting averaged spectra, which were retrieved from at least 3 repetitions per sample.

2.3.3. Solid-state nuclear magnetic resonance (NMR)

Solid-state ^{13}C Cross-Polarization Magic Angle Spinning (CP-MAS) spectra were collected at 125.76 MHz on an Avance 500 MHz NMR Spectrometer (Bruker Italia s.r.l., Milan, Italy) as thoroughly described elsewhere (Rovera et al., 2023). All the samples were first packed in Zirconia (ZrO_2) rotors, closed with Kel-F caps (50 μL internal volume), and analyzed by fixing the MAS rate at 10 kHz. The crystallinity index ($C.I._{NMR}$, in %) of cellulose samples was estimated by applying the Global Spectral Deconvolution (GSD) analysis algorithm supported by the MestReNova v. 14.1.2 software (Mestrelab Research S.L., Santiago de Compostela, Spain).

2.3.4. X-ray diffraction (XRD)

Cellulose powder was analyzed using a MiniFlex600 diffractometer (Rigaku, Tokyo, Japan). The data were collected using Cu Kα radiation at the following operating conditions: 40 kV, 15 mA, 2θ range 5–50°, step size 0.02°, scan speed 1.00°/min. X-ray patterns were evaluated using SmartLab Studio-II software. The crystallinity index ($C.I._{XRD}$, in %) was calculated from the height ratio between the intensity of the crystalline peak and total intensity after subtraction of the background signal measured without cellulose (Park et al., 2010). The so-obtained $C.I._{XRD}$ values were then compared with those determined by NMR.

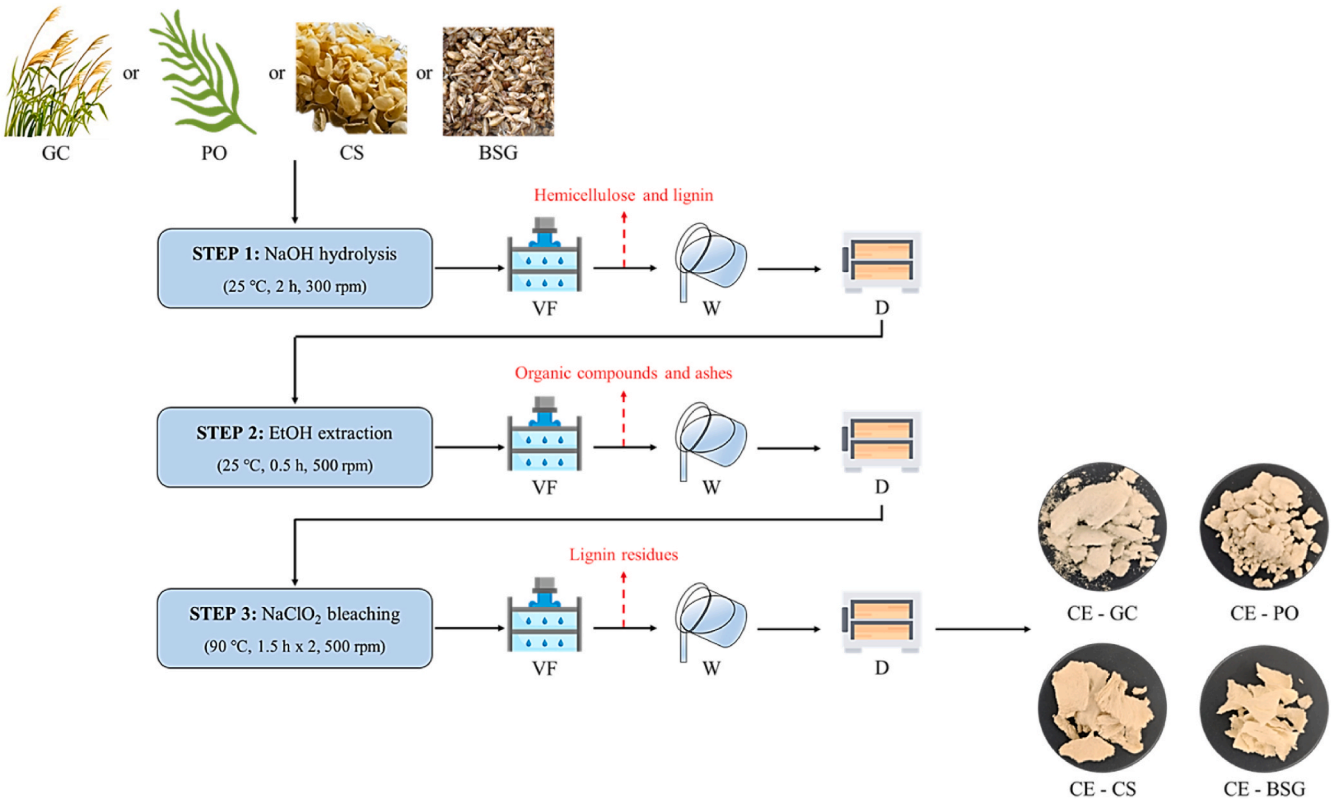

Fig. 1. Representative sketch of the cellulose extraction protocol applied to all tested biomasses. Legend: GC – giant cane, PO – *Posidonia oceanica* seagrass, CS – coffee silverskin, BSG – brewer's spent grain, VF – vacuum filtration, W – washing, D – drying, CE – cellulosic extract.

2.3.5. Scanning electron microscopy (SEM)

The morphological features of cellulose extracted through the proposed protocol were evaluated using a table-top scanning electron microscope (SNE-ALPHA, SEC Co., Korea) working at an accelerating voltage of 10 kV. Powdered cellulose was first mounted on metallic stubs covered with carbon tape and subsequently metalized with gold to an approximate thickness of 5 nm using an MCM-100 ion sputter coater (SEC Co., Korea). SEM micrographs were collected at 1000× , 5000× , and 15000× magnifications.

2.4. Statistical analysis

Processing of biomasses and further analysis were performed in triplicate and the results were reported as means ± standard deviations. Where applicable, differences among mean values were assessed by one-way analysis of variance (ANOVA), executed with SPSS 20 (SPSS IBM., Chicago, USA) statistical package. Statistically significant differences ($p < 0.05$) were determined by the Tukey test.

3. Results and discussion

3.1. Extraction yield

GC, PO, CS, and BSG underwent the three-step process previously depicted in Fig. 1 to eventually recover the cellulosic biomass. Once dried, cellulose was immediately weighed to assess the yield of extraction. As shown in Table 2, for the four biomasses the yield was comparable to the theoretical cellulose content (see Table 1), thus demonstrating that the applied chemical procedure was effective in the recovery of cellulose. These data align with those obtained in previous works on the multi-step extraction of cellulose from the same biomasses as in the present study (Ballesteros et al., 2014; Camacho-Nunez et al., 2023; Pires et al., 2022; Rovera et al., 2023; Tarchoun et al., 2019; Vallejo et al., 2021).

3.2. FT-IR spectroscopy

The FT-IR spectra (Fig. 2a) are dominated by seven characteristic absorption peaks of cellulose, according to the previous assignments by Tarchoun et al. (2019). In particular, the peaks at 3330 cm^{-1} and 2923 cm^{-1} are associated with the stretching vibration of the O-H bonds of the primary/secondary hydroxyl groups and the C-H bonds assigned to the cellulose crystalline order, respectively. The absorption peak at 1650 cm^{-1} was attributed to the OH deformational vibration of the absorbed water. The subtle peak at 1430 cm^{-1} is attributed to the CH_2 bending vibration. The peaks within the range of 1165–1110 cm^{-1} correspond to the C-O-C stretching and skeletal vibration of the pyranose ring in cellulose. At last, the stretching vibration of the C-O bonds generates the peak at 1060 cm^{-1}. Fig. 2a shows high similarity among spectra, thus suggesting an almost identical chemical composition of cellulose extracted from the four biomasses. A good correspondence with spectra derived from bacterial cellulose and filter paper was also observed. Interestingly, only the FT-IR spectrum of the CE-PO sample exhibited a

Table 2
Yield (Y_C) and crystallinity index (C.I.), calculated using both NMR and XRD data, of cellulose extracts from tested biomasses. Results are expressed as mean ± standard deviation. In the case of yield, different superscript letters express significant differences among mean values as a function of substrate ($p < 0.05$). Legend: % DW_b = percentage of dry weight biomass.

Sample	Y_C (% DW_b)	$C.I._{NMR}$ (%)	$C.I._{XRD}$ (%)
CE-GC	36.4 ± 2.6^b	41.74	68.06
CE-PO	38.6 ± 3.9^b	34.93	49.55
CE-CS	23.1 ± 1.4^a	33.26	56.65
CE-BSG	22.2 ± 0.8^a	32.25	58.43

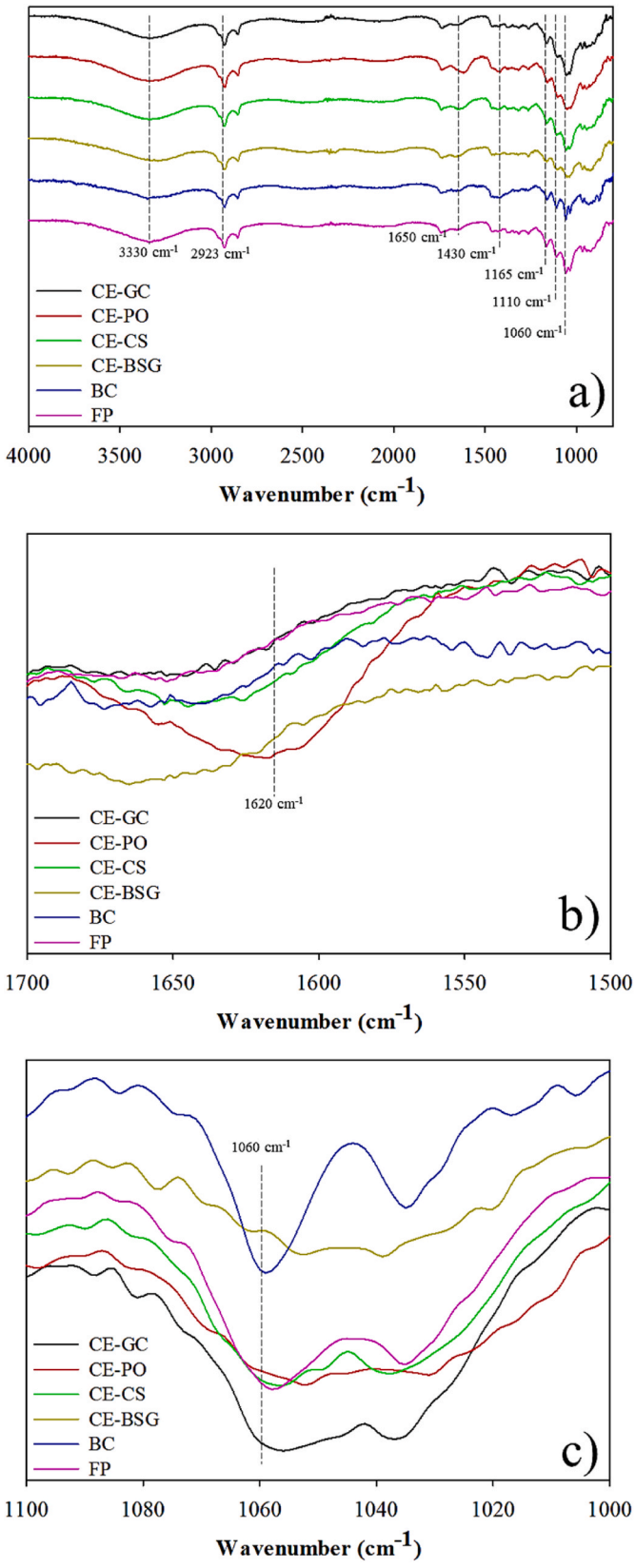

Fig. 2. FT-IR spectra of CE-GC, CE-PO, CE-CS, and CE-BSG samples within 4000–800 cm^{-1} (a), 1700–1500 cm^{-1} (b), and 1100–1000 cm^{-1} (c). The spectra of bacterial cellulose (BC) and filter paper (FP) (Whatman grade 3 MM) are also reported.

peak at around 1620 cm^{-1} (Fig. 2b), which can be ascribed to the C=O stretching vibration in esters and other carbonyl-type groups in monomers from both lignin (e.g., ferulic and *p*-coumaric acids) and hemicellulose (e.g., acetyl and uronic ester groups) chains (Rovera et al., 2023; Tarchoun et al., 2019). Applying the same extraction protocol, the higher percentage of lignin and hemicellulose in PO biomass (Table 1) might have contributed to a greater level of impurities in the extracted cellulose. Additional experiments are necessary to understand the effect of the microstructural arrangement of the investigated matrices on the purity degree of cellulose after the extraction procedure. This would allow to optimize the extraction parameters to minimize the presence of polluting molecules in the final extract.

Looking at the spectra of Fig. 2c, the more pronounced peak at 1060 cm^{-1} shown by the reference substrates and only partially by the CE-GC sample can be attributed to their slightly greater purity as compared to cellulose extracted from the plant-based biomasses (Camacho-Nunez et al., 2023). Analogous conclusions were drawn by Garnett et al. (2024), who explored the feasibility of using mixed food wastes from a local restaurant as a substrate for cellulose extraction. FT-IR spectroscopy underscored a clear overlapping between the FT-IR spectra of cellulose from restaurant wastes and those obtained from commercial cellulose, though some impurities related to residual lignin fragments were detected.

3.3. NMR spectroscopy

The ^{13}C CP MAS NMR spectra of CE-GC, CE-PO, CE-CS, and CE-BSG samples are displayed in Fig. 3. All the samples exhibited the typical pattern of pure cellulose, with signals at 105 ppm (C_1), 80–90 ppm (C_4 crystalline-amorphous region), 70 ppm ($C_{2,3,5}$ fraction), and 60–99 ppm (C_6 crystalline region). This is in full agreement with previous findings on the extraction of cellulose from agri-food wastes, including orange peels (de Castro et al., 2024), corncob and garlic stalks (Rovera et al., 2023), rice husk (Nguyen et al., 2022), and bitter cucumber seeds (Kouadri & Satha, 2018). Interestingly, the weak signals detected at 175.5 ppm (for CE-PO, CE-CS, and CE-BSG) and within the 30–34 ppm range (only for CE-PO and CE-BSG) are due to carbonyl groups and the methylene groups adjacent to them of organic compounds other than cellulose (Sejati et al., 2022). This foretells the presence of traces of hemicellulose and lignin still contaminating the cellulose samples after extraction, thereby confirming the previous conclusion drawn from the FT-IR analysis (i.e., the extraction protocol does not yield pure cellulose). In a similar fashion, Choi et al. (2018) observed subtle peaks in the NMR spectrum of graviola leaf-derived cellulose at 30 ppm and 155 ppm, being presumably linked to unremoved non-cellulosic materials after purification.

The deconvolution of NMR spectra (Fig. 3) was advantageously used to estimate the crystallinity index ($C.I._{NMR}$) of cellulose obtained from the tested biomasses. As shown in Table 2, $C.I._{NMR} < 50\%$ was detected for all the samples, thus indicating that the amorphous domains prevailed over the crystalline ones. Several authors assessed the crystallinity index of cellulose extracted from plant residues and agri-food wastes and contrasting results were collected. In agreement with our findings, $C.I._{NMR}$ values of ≈45%, 35%, and 40% were obtained for cellulose from sugarcane bagasse (Bernardinelli et al., 2015), almond shell (Modica et al., 2020) and hop stems (Kanai et al., 2021), respectively. On the other hand, cellulose extracted from eggplant residues (Bahloul et al., 2021) and chemo-enzymatic treated citrus waste (Mariño et al., 2015) was found to reach crystallinity indexes greater than 50%. These discrepancies with our results could be attributed to the presence of unremoved lignin and hemicellulose traces in the extracted cellulose, which are known to curb the overall crystallinity of the final extract (Jang et al., 2023). However, to confirm these hypotheses and to better characterize the obtained cellulose, additional analyses are necessary.

3.4. XRD spectroscopy

The XRD diffractograms of CE-GC, CE-PO, CE-CS, and CE-BSG are displayed in Fig. 4. All the samples are characterized by three main peaks centered at approximately $2\theta = 16.2°$, 22.5°, and 34.8°, which are respectively associated with 1–10/100, 002, and 004 crystal planes of cellulose I_β, the predominant polymorph present in higher plants (Cozzolino et al., 2014; French, 2014). Only for the sample CE-CS, a minor shoulder at $2\theta = 15 - 17°$ separates signals from crystal planes with Miller indices of (1–10) and (110). On the other hand, an overlap of these signals generates the broader peak at $2\theta = 16.2°$ for CE-GC, CE-PO, and CE-BSG samples, as previously observed (Camacho-Nunez et al., 2023; Gomez Hoyos et al., 2020; Ren et al., 2019).

Noteworthy, higher C.I. values were detected when applying the XRD peak height method compared to the NMR C4 peak separation technique (Table 2). This result fits with the established overestimation of C.I. provided by the XRD peak height method (Park et al., 2010), thus confirming the greater calculation accuracy granted by the deconvolution methods based on the NMR analysis. Accordingly, Mariño et al. (2015) claimed that the absolute values of $C.I._{XRD}$ must be taken with caution, because of the inherent approximation of the amorphous

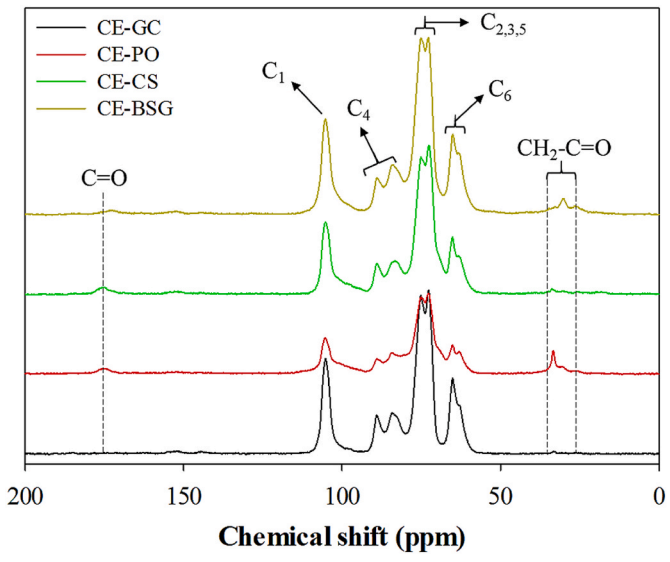

Fig. 3. ^{13}C CP MAS NMR spectra of CE-GC, CE-PO, CE-CS, and CE-BSG samples.

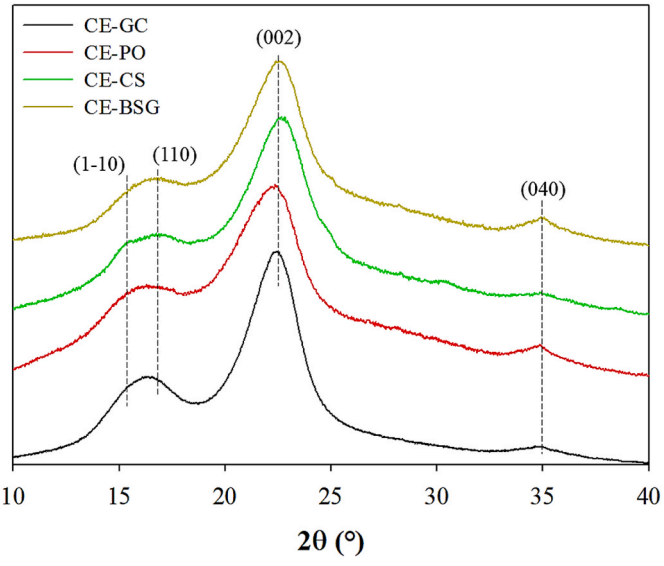

Fig. 4. XRD diffraction patterns of CE-GC, CE-PO, CE-CS, and CE-BSG samples.

domain within the cellulosic network. Expediently, the XRD peak height method is a reliable tool when the goal is to highlight relative differences in crystallinity among cellulose samples extracted through the same purification process (Fig. 1), as done in this study and in a recent work (Wang et al., 2024), where the crystallinity of cellulose from tea residues was found to range between 47.4% and 52.6%.

3.5. SEM analyses

SEM images of CE-GC, CE-PO, CE-CS, and CE-BSG samples are depicted in Fig. 5. A fibril-like morphology, typical of microcrystalline cellulose with a mostly rough surface, was observed for all cellulosic samples, in line with recent works on cellulose extraction from date palm waste, sweet sorghum, and residues from black, green, and Pu-erh teas (Raza et al., 2022; Ren et al., 2019; Wang et al., 2024). As disclosed by micrographs at 1000× magnification, fibrils are organized in bundles rather than in individual units, which could be due to the presence of residual lignin acting as a glue in the lignocellulosic structure (Camacho-Nunez et al., 2023). This observation seems to confirm that the biomass obtained through the protocol proposed in this work (Fig. 1) is represented by high-purity cellulose still containing residual impurities probably represented by lignin and hemicellulose. SEM pictures taken at higher magnifications unveiled a width ranging between 6 μm and 13 μm for fibrils which, in turn, are organized into a stack of microfibrils approaching sizes well below 1 μm (see the "CE-CS – 15000× " image in Fig. 5). These findings are supported by some evidence in the literature. For instance, Zeleke et al. (2022) applied a purification process based on toluene-ethanol dewaxing, NaOH treatment, and H_2SO_4/H_2O_2-catalyzed bleaching to extract microcrystalline cellulose from the outer skin-isolated coffee husk. The authors pinpointed the key role played by the two-cycle bleaching step in yielding fibrils of 2–3 μm in diameter. Nuruddin et al. (2011) implemented an integrated biorefinery scheme to extract cellulose microfibrils from rice straw, wheat straw, corn stalks, and dhaincha. The latter exhibited average diameters of 8.7, 9.3, 6.6, and 6.8 μm following SEM analyses, thus showing full correspondence with our results (Fig. 5).

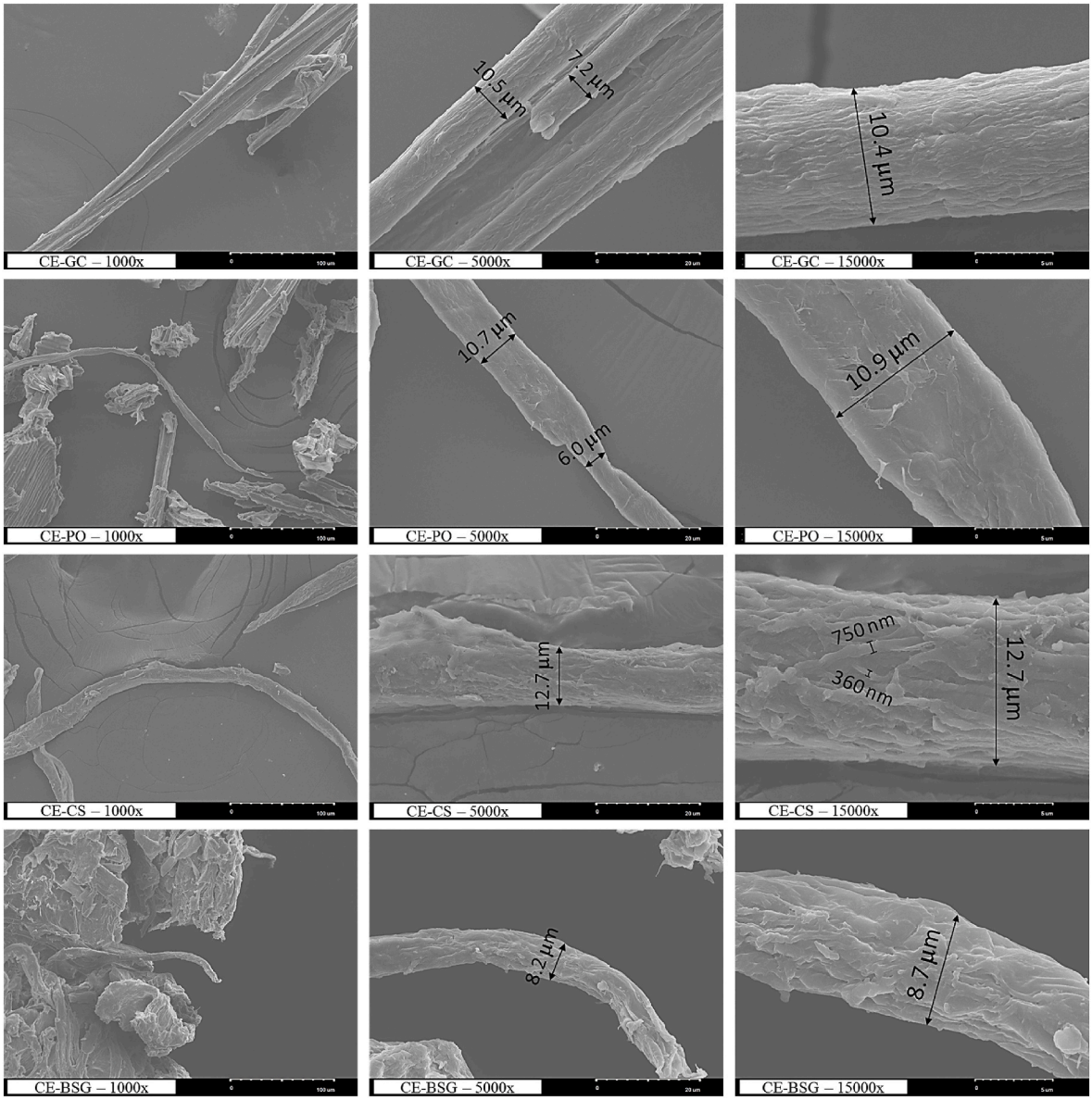

Fig. 5. SEM micrographs (1000× , 5000× , and 15000× magnification) of cellulosic extracts obtained from tested biomasses. The size of cellulosic fibrils and microfibrils was also reported.

3.6. Soft-chemicals extraction process vs. conventional methods

Table 3 provides a comparison between the soft-chemical extraction method developed in this work and the methods found in the literature for the extraction of cellulose from the same biomasses, that are, GC, PO, CS, and BSG. In particular, chemicals/solvents load per g of processed raw material, overall extraction time, as well as yield and crystallinity of extracted cellulose were put under the spotlight. Lack of adequate information made impossible any comparison in terms of cellulose purity and cost-effectiveness of the processes. Regardless of the biomass, similar values were found in terms of yield and crystallinity of cellulose between our method and the methods used by other scientists. However, some advantages over conventional techniques can be outlined. First, neither hazardous solvents (e.g., toluene, xylene) nor strong acids (e.g., H_2SO_4 and HNO_3) were involved in this work to boost cellulose extraction. Second, a significant reduction in solvent amount, processing temperatures, and overall extraction time was attained. The latter parameters are known to affect dramatically the operative costs associated with the lignocellulosic biorefinery processes (Yogalakshmi et al., 2023). Therefore, pending future environmental and economic evaluations, we can supposedly claim that the newly designed cellulose extraction protocol outperforms the conventional ones as far as the sustainability aspects are concerned.

4. Conclusions

The SWOT analysis of Fig. 6 underscores the potential of the protocol set in our work for the extraction of cellulose from biomasses of different origins and compositions. The cascade method used in our study can perform better than conventional processes in terms of efficiency, versatility, and environmental impact. On the other hand, there are still some hurdles to be addressed, namely the need for high-energy demanding pre-treatments of the biomasses and the presence – though reduced – of polluting chemicals. A great opportunity to replace commonly used biomasses for cellulose extraction (e.g., wood and cotton) with agri-waste feedstocks is also evidenced, thus paving the way towards a "circular economy" model. Eventually, the establishment of an easy, economically convenient, and continuous supply chain of raw materials, together with the unavoidable post-processing of achieved cellulose to fabricate marketable products, represent the main challenges to be considered for the potential scale-up of the adopted extraction process.

In conclusion, additional steps ahead are necessary to:

i) explore other biomasses for cellulose recovery to ensure a large availability of the raw materials;
ii) investigate new options for the extraction protocol using more eco-friendly chemicals;
iii) perform a techno-economical assessment of the proposed strategy as compared to conventional extraction methods;
iv) carry out a quantitative analysis of the environmental impact of the proposed protocol;
v) execute a market analysis for the achieved cellulosic residues;

Table 3
Yield and crystallinity of cellulose recovered from GC, PO, CS, and BSG, both found in this work and retrieved from recent literature findings.

Biomass	Extraction protocol	Chemical load per g of biomass	Overall extraction time	Yield (%)	Crystallinity (%)	Reference
GC	Soxhlet extraction with toluene/ethanol 2:1 (v/v) (RT) + bleaching with 1.4% (w/v) $NaClO_2$ solution (70 °C) + delignification with 5% (w/v) KOH solution (RT)	80 mL toluene/ethanol + 1.1 g $NaClO_2$ + 4.52 g KOH	55 h	17.7	50.5	Martínez-Sanz et al. (2018)
	Soaking in 1N NaOH solution (RT)	N.R.	10 days	34.0	51.5	Suárez et al. (2022)
	Delignification with 0.5N NaOH solution (RT) + hydrolysis with nitric-chromic acids mixture (RT) + soxhlet extraction with toluene/ethanol 2:1 (v/v) (RT)	N.R.	46 h	24.0	81.3	Gaikwad et al. (2023)
	Delignification with 20% (w/v) NaOH solution (RT) + extraction with xylene (RT) + bleaching with 1% (w/v) $NaClO_2$ solution (90 °C)	20 g NaOH + 14 mL xylene + 0.25 g $NaClO_2$	4 h	39.1	75.0	Rovera et al. (2023)
	Delignification with 5% (w/v) NaOH solution (RT) + extraction with 95% (v/v) ethanol solution (RT) + bleaching with 1% (w/v) $NaClO_2$ solution (90 °C)	5 g NaOH + 14 mL ethanol + 0.5 g $NaClO_2$	5.5 h	36.4	68.1	This work
PO	Soxhlet extraction with toluene/ethanol 2:1 (v/v) (RT) + bleaching with 1.7% (w/v) $NaClO_2$ solution (70 °C) + delignification with 5% (w/v) KOH solution (RT)	22 mL toluene/ethanol + 3.6 g $NaClO_2$ + 2.5 g KOH	39 h	32.5	60.5	Tarchoun et al. (2019)
	Soxhlet extraction with toluene/ethanol 2:1 (v/v) (RT) + bleaching with 1.4% (w/v) $NaClO_2$ solution (70 °C) + delignification with 5% (w/v) KOH solution (RT)	200 mL toluene/ethanol + 3.2 g $NaClO_2$ + 9.4 g KOH	55 h	24.0	51.4	Benito-Gonzales et al. (2018)
	Delignification with 5% (w/v) NaOH solution (RT) + extraction with 95% (v/v) ethanol solution (RT) + bleaching with 1% (w/v) $NaClO_2$ solution (90 °C)	5 g NaOH + 14 mL ethanol + 0.5 g $NaClO_2$	5.5 h	38.6	49.5	This work
CS	Soxhlet extraction with n-hexane (RT) + delignification with 0.1N NaOH solution (60 °C) + bleaching with 10% (w/v) H_2O_2 solution (45 °C)	N.R.	60 h	24.8	56.0	Alghooneh et al. (2017)
	Delignification with 5% (w/v) NaOH solution (RT) + extraction with 95% (v/v) ethanol solution (RT) + bleaching with 1% (w/v) $NaClO_2$ solution (90 °C)	5 g NaOH + 14 mL ethanol + 0.5 g $NaClO_2$	5.5 h	23.1	56.6	This work
BSG	Extraction with 80% (v/v) ethanol solution (RT) + hydrolysis with 4.7% (w/v) H_2SO_4 (45 °C) + delignification with 4N NaOH solution (RT) + bleaching with 5% (w/v) H_2O_2 solution (RT)	16 mL ethanol + 0.47 g H_2SO_4 + 1.6 g NaOH + 0.5 mL H_2O_2	58 h	5.7	N.R.	Vellingiri et al. (2014)
	Hydrolysis with HNO_3 (80 °C) + delignification with 2% (w/v) NaOH solution (80 °C) + bleaching with 5% (w/v) H_2O_2 solution (70 °C)	0.9 g HNO_3 + 0.4 g NaOH + 1 g H_2O_2	3.5 h	28.0	63.0	Camacho-Nunez et al. (2023)
	Delignification with 5% (w/v) NaOH solution (RT) + extraction with 95% (v/v) ethanol solution (RT) + bleaching with 1% (w/v) $NaClO_2$ solution (90 °C)	5 g NaOH + 14 mL ethanol + 0.5 g $NaClO_2$	5.5 h	22.2	58.4	This work

Legend: RT = room temperature, N.R. = not reported.

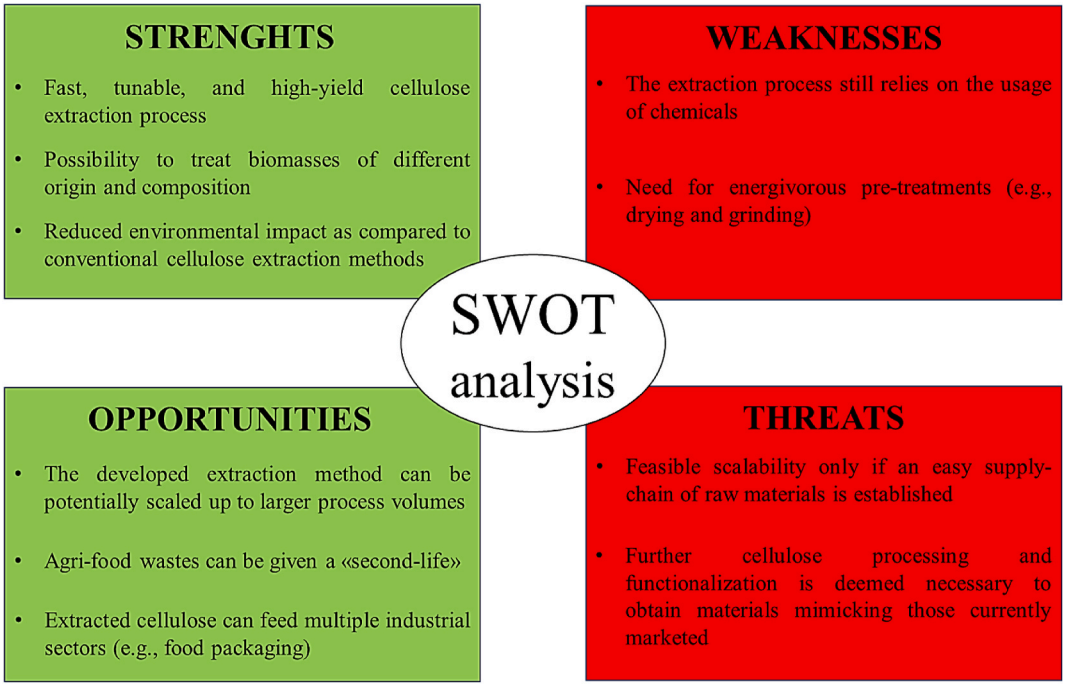

Fig. 6. SWOT analysis on the application of the soft-chemical cellulose extraction process developed in this work.

vi) evaluate cellulose-derived forms (e.g., microfibrils and nanocrystals) as fillers or coating agents for food packaging to verify the feasibility of replacing conventional fossil-based plastics with more sustainable materials.

Funding

This study was carried out within the Agritech National Research Center and received funding from the European Union Next-Generation EU (PIANO NAZIONALE DI RIPRESA E RESILIENZA (PNRR) – MISSIONE 4 COMPONENTE 2, INVESTIMENTO 1.4 – D.D. 1032 June 17, 2022, CN00000022). T. Bellesia's PhD contract was funded by the European Union – FSE, Research & Innovation 2014–2020 National Operative Program (DOT1315775-6 and 15-G-13883-1) and Fedrigoni Spa (FED_20220718_0030920126).

CRediT authorship contribution statement

Tommaso Bellesia: Writing – original draft, Methodology, Investigation, Formal analysis, Data curation, Conceptualization. **Daniele Carullo:** Writing – original draft, Methodology, Investigation, Formal analysis, Data curation, Conceptualization. **Andrea Fachin:** Writing – review & editing, Formal analysis. **Enrico Caneva:** Formal analysis. **Stefano Farris:** Writing – review & editing, Supervision, Project administration, Methodology, Funding acquisition, Conceptualization.

Declaration of competing interest

The authors declare that they have no known competing financial interests or personal relationships that could have appeared to influence the work reported in this paper.

Data availability

Data will be made available on request.

Acknowledgments

Dr. Massimo Zonca is greatly acknowledged for sharing ideas and fruitful discussions.

Appendix A. Supplementary data

Supplementary data to this article can be found online at https://doi.org/10.1016/j.fbio.2024.105141.

References

Alghooneh, A., Mohammad Amini, A., Behrouzian, F., & Razavi, S. M. A. (2017). Characterisation of cellulose from coffee silverskin. *International Journal of Food Properties, 20*, 2830–2843. https://doi.org/10.1080/10942912.2016.1253097

Apicella, A., Adiletta, G., Albanese, D., Di Matteo, M., & Incarnato, L. (2021). Biodegradable films based on poly(lactic acid) coatings and natural olive-wastewater extracts for active food packaging. *Chemical Engineering Transactions, 87*, 85–90. https://doi.org/10.3303/CET2187015

Asgher, M., Qamar, S. A., Bilal, M., & Iqbal, H. M. N. (2020). Bio-based active food packaging materials: Sustainable alternative to conventional petrochemical-based packaging materials. *Food Research International, 137*, Article 109625. https://doi.org/10.1016/j.foodres.2020.109625

Bahloul, A., Kassab, Z., El Bouchti, M., Hannache, H., Qaiss, A. E. K., Oumam, M., & El Achaby, M. (2021). Micro-and nano-structures of cellulose from eggplant plant (*Solanum melongena L*) agricultural residue. *Carbohydrate Polymers, 253*, Article 117311. https://doi.org/10.1016/j.carbpol.2020.117311

Balata, G., & Tola, A. (2018). Cost-opportunity analysis of the use of *Posidonia oceanica* as a source of bio-energy in tourism-oriented territories. The case of Alghero. *Journal of Cleaner Production, 172*, 4085–4098. https://doi.org/10.1016/j.jclepro.2017.02.072

Ballesteros, L. F., Teixeira, J. A., & Mussatto, S. I. (2014). Chemical, functional, and structural properties of spent coffee grounds and coffee silverskin. *Food and Bioprocess Technology, 7*, 3493–3503. https://doi.org/10.1007/s11947-014-1349-z

Bangar, S. P., Kajla, P., & Ghosh, T. (2023). Valorization of wheat straw in food packaging: A source of cellulose. *International Journal of Biological Macromolecules, 227*, 762–776. https://doi.org/10.1016/j.ijbiomac.2022.12.199

Beji, E., Keshk, S. M. A. S., Douiri, S., Charradi, K., Ben Hassen, R., Gtari, M., Attia, H., & Ghorbe, D. (2023). Bioactive film based on chitosan incorporated with cellulose and aluminum chloride for food packaging application: Fabrication and characterization. *Food Bioscience, 53*, Article 102678. https://doi.org/10.1016/j.fbio.2023.102678

Benito-González, I., López-Rubio, A., & Martínez-Sanz, M. (2018). Potential of lignocellulosic fractions from *Posidonia oceanica* to improve barrier and mechanical properties of bio-based packaging materials. *International Journal of Biological Macromolecules, 118*, 542–551. https://doi.org/10.1016/j.ijbiomac.2018.06.052

Bernardinelli, O. D., Lima, M. A., Rezende, C. A., Polikarpov, I., & de Azevedo, E. R. (2015). Quantitative ^{13}C MultiCP solid-state NMR as a tool for evaluation of

cellulose crystallinity index measured directly inside sugarcane biomass. *Biotechnology for Biofuels, 8*, 110. https://doi.org/10.1186/s13068-015-0292-1
Camacho-Núnez, L., Jurado-Contreras, S., La Rubia, M. D., Navas-Martos, F. J., & Rodríguez-Liebana, J. A. (2023). Cellulose-based upcycling of brewer's spent grains: Extraction and acetylation. *Journal of Polymers and the Environment, 32*, 1–14. https://doi.org/10.1007/s10924-023-03137-w
Carullo, D., Casson, A., Rovera, C., Ghaani, M., Bellesia, T., Guidetti, R., & Farris, S. (2023). Testing a coated PE-based mono-material for food packaging applications: An in-depth performance comparison with conventional multi-layer configurations. *Food Packaging and Shelf Life, 39*, Article 101143. https://doi.org/10.1016/j.fpsl.2023.101143
Castro, L. E. N., & Colpini, L. M. S. (2021). All-around characterization of brewers' spent grain. *European Food Research and Technology, 247*, 3013–3021. https://doi.org/10.1007/s00217-021-03860-5
Choi, M., Kang, Y.-R., Lim, I.-S., & Chang, Y. H. (2018). Structural characterization of cellulose obtained from extraction wastes of graviola (*Annona muricata*) leaf. *Preventive Nutrition and Food Science, 26*, 166–170. https://doi.org/10.3746/pnf.2018.23.2.166
Corno, L., Lonati, S., Riva, C., Pilu, R., & Adani, F. (2016). Giant cane (*arundo Donax* L.) can substitute traditional energy crops in producing energy by anaerobic digestion, reducing surface area and costs: A full-scale approach. *Bioresource Technology, 218*, 826–832. https://doi.org/10.1016/j.biortech.2016.07.050
Corno, L., Pilu, R., & Adani, F. (2014). *Arundo donax* L.: A non-food crop for bioenergy and bio-compound production. *Biotechnology Advances, 32*, 1535–1549. https://doi.org/10.1016/j.biotechadv.2014.10.006
Cozzolino, C. A., Cerri, G., Brundu, A., & Farris, S. (2014). Microfibrillated cellulose (MFC): Pullulan bionanocomposite films. *Cellulose, 21*, 4323–4335. https://doi.org/10.1007/s10570-014-0433-x
de Castro, S. C., Stanisic, D., & Tasic, L. (2024). Sequential extraction of hesperidin, pectin, lignin, and cellulose from orange peels: Towards valorization of agro-waste. *Biofuels Bioproducts and Biorefining, 18*, 804–817. https://doi.org/10.1002/bbb.2606
El-Sayed, S. M., & Youssef, A. M. (2023). Eco-friendly biodegradable nanocomposite materials and their recent use in food packaging applications: A review. *RSC – Sustainable Food Technology, 1*, 215. https://doi.org/10.1039/d2fb00021k
FAOSTAT. (2022). Crops and livestock products. Available online at: https://www.fao.org/faostat/en/#data/QC. (Accessed 29 February 2024).
Forcina, A., Petrillo, A., Travaglioni, M., di Chiara, S., & De Felice, F. (2023). A comparative life cycle assessment of different spent coffee ground reuse strategies and a sensitivity analysis for verifying the environmental convenience based on the location of sites. *Journal of Cleaner Production, 385*, Article 135727. https://doi.org/10.1016/j.jclepro.2022.135727
French, A. D. (2014). Idealized powder diffraction patterns for cellulose polymorphs. *Cellulose, 21*, 885–896. https://doi.org/10.1007/s10570-013-0030-4
Gaikwad, A., Debnath, K., & Gupta, M. K. (2023). Effects of alkaline-acid treatment on the physiochemical attributes of natural cellulosic fiber of *Arundo donax* L. *Journal of Applied Polymer Science, 140*, Article e54724. https://doi.org/10.1002/app.54724
Garnett, M. T., Kumar, H. K. S., Beckingham, B. S., & Alexander, S. L. M. (2024). Extraction of cellulose from restaurant food waste. *RSC Sustainability, 2*, 170. https://doi.org/10.1039/d3su00192j
Gomez Hoyos, C., Marquez, P. M., Velez, L. P., Guerra, A. S., Eceiza, A., Urbina, L., Velasquez-Cock, J., Ganan Rojo, P., Velez Acosta, L., & Zuluaga, R. (2020). Cocoa shell: An industrial by-product for the preparation of suspensions of holocellulose nanofibers and fat. *Cellulose, 27*, 10873–10884. https://doi.org/10.1007/s10570-020-03222-6
Huang, K., Maltais, A., Liu, J., & Wang, Y. (2022). Wood cellulose films regenerated from NaOH/urea aqueous solution and treated by hot pressing for food packaging application. *Food Bioscience, 50*(Part B), Article 102177. https://doi.org/10.1016/j.fbio.2022.102177
Iadecola, R., Ciccoritti, R., Ceccantoni, B., Bellincontro, A., & Amoriello, T. (2022). Optimization of phenolic compound extraction from brewers' spent grain using ultrasound technologies coupled with response surface methodology. *Sustainability, 14*, 3309. https://doi.org/10.3390/su14063309
Iftikhar, T., Majeed, H., Altaf, F., & Khalid, A. (2024). Upcycling of the industrial waste as a sustainable source of axenic fungal strain (*Aspergillus oryzae*) for scale up enzymatic production with kinetic analysis and Box-Behnken design application. *Zeitschrift fur Physikalische Chemie, 238*, 115–131. https://doi.org/10.1515/zpch-2023-0311
Jang, S.-K., Jeong, H., & Choi, I.-G. (2023). The effect of cellulose crystalline structure modification on glucose production from chemical-composition-controlled biomass. *Sustainability, 15*, 5869. https://doi.org/10.3390/su15075869
Kanai, N., Nishimura, K., Umetani, S., Saito, Y., Saito, H., Oyama, T., & Kawamura, I. (2021). Upcycling of waste hop stems into cellulose nanofibers: Isolation and structural characterization. *ACS Agricultural Science and Technology, 1*, 347–354. https://doi.org/10.1021/acsagscitech.1c00041
Khan, R., Jolly, R., Fatima, T., & Shakir, M. (2022). Extraction processes for deriving cellulose: A comprehensive review on green approaches. *Polymers for Advanced Technologies, 33*, 2069–2090. https://doi.org/10.1002/pat.5678
Khezerlou, A., Tavassoli, M., Sani, M. A., Mohammadi, K., Ehsani, A., & McClements, D. J. (2021). Application of nanotechnology to improve the performance of biodegradable biopolymer-based packaging materials. *Polymers, 13*, 4399. https://doi.org/10.3390/polym13244399
Kouadri, I., & Satha, H. (2018). Extraction and characterization of cellulose and cellulose nanofibers from *Citrullus colocynthis* seeds. *Industrial Crops and Products, 124*, 787–796. https://doi.org/10.1016/j.indcrop.2018.08.051
Kumar, S., Mukherjee, A., & Dutta, J. (2020). Chitosan based nanocomposite films and coatings: Emerging antimicrobial food packaging alternatives. *Trends in Food Science & Technology, 97*, 196–209. https://doi.org/10.1016/j.tifs.2020.01.002
Liu, X., Sun, H., & Leng, X. (2023). Coffee silverskin cellulose-based composite film with natural pigments for food packaging: Physicochemical and sensory abilities. *Foods, 12*, 2839. https://doi.org/10.3390/foods12152839
Majeed, H., Iftikhar, T., Ahmad, K., Qureshi, K., Tabinda, Altaf, F., Iqbal, A., Ahmad, S., & Khalid, A. (2023). Bulk industrial production of sustainable cellulosic printing fabric using agricultural waste to reduce the impact of climate change. *International Journal of Biological Macromolecules, 253*, Article 126885. https://doi.org/10.1016/j.ijbiomac.2023.126885
Mariño, M., Lopes da Silva, L., Durán, N., & Tasic, L. (2015). Enhanced materials from nature: Nanocellulose from citrus waste. *Molecules, 20*, 5908–5923. https://doi.org/10.3390/molecules20045908
Martínez-Sanz, M., Erboz, E., Fontes, C., & López-Rubio, A. (2018). Valorization of *Arundo donax* for the production of high performance lignocellulosic films. *Carbohydrate Polymers, 199*, 276–285. https://doi.org/10.1016/j.carbpol.2018.07.029
Modica, A., Rosselli, S., Catinella, G., Sottile, F., Catania, C. A., Cavallaro, G., Lazzara, G., Botta, L., Spinella, A., & Bruno, M. (2020). Solid state ^{13}C-NMR methodology for the cellulose composition studies of the shells of *Prunus dulcis* and their derived cellulosic materials. *Carbohydrate Polymers, 240*, Article 116290. https://doi.org/10.1016/j.carbpol.2020.116290
Mussatto, S. I. (2014). Brewer's spent grain: A valuable feedstock for industrial applications. *Journal of the Science of Food and Agriculture, 94*, 1264–1275. https://doi.org/10.1002/jsfa.6486
Nguyen, N. T., Tran, N. T., Phan, T. P., Nguyen, A. T., Nguyen, M. X. T., Nguyen, N. N., Ko, Y. H., Nguyen, D. H., Van, T. T. T., & Hoang, D. Q. (2022). The extraction of lignocelluloses and silica from rice husk using a single biorefinery process and their characteristics. *Journal of Industrial and Engineering Chemistry, 108*, 150–158. https://doi.org/10.1016/j.jiec.2021.12.032
Nuruddin, N., Chowdhury, A., Haque, S. A., Rahman, M., Farhad, S. F., Sarwar Jahan, M., & Quaiyyum, A. (2011). Extraction and characterization of cellulose microfibrils from agricultural wastes in an integrated biorefinery initiative. *Cellulose Chemistry and Technology, 45*, 347–354.
Orqueda, M. E., Méndez, D. A., Martínez-Abad, A., Zampini, C., Torres, S., Isla, M. I., Lopez-Rubio, A., & Fabra, M. J. (2022). Feasibility of active biobased films produced using red chilto wastes to improve the protection of fresh salmon fillets via a circular economy approach. *Food Hydrocolloids, 133*, Article 107888. https://doi.org/10.1016/j.foodhyd.2022.107888
Overturf, E., Pezzutto, S., Boschiero, M., Ravasio, N., & Monegato, A. (2021). The CirCo (circular coffee) project: A case study on valorization of coffee silverskin in the context of circular economy in Italy. *Sustainability, 13*, 9069. https://doi.org/10.3390/su13169069
Park, S., Baker, J. O., Himmel, M. E., Parilla, P. A., & Johnson, D. K. (2010). Cellulose crystallinity index: Measurement techniques and their impact on interpreting cellulase performance. *Biotechnology for Biofuels, 3*, 10. https://doi.org/10.1186/1754-6834-3-10
Picot-Allain, M. C. N., & Emmambux, M. N. (2021). Isolation, characterization, and application of nanocellulose from agro-industrial by-products: A review. *Food Reviews International, 39*, 941–969. https://doi.org/10.1080/87559129.2021.1928689
Pietrosanto, A., Apicella, A., Scarfato, P., Incarnato, L., & Di Maio, L. (2022). Development of novel blown shrink films from poly(lactide)/poly(butylene-adipate-co-terephthalate) blends for sustainable food packaging applications. *Polymers, 14*, 2759. https://doi.org/10.3390/polym14142759
Pires, J. R. A., Souza, V. G. L., Gomes, L. A., Coelhoso, I. M., Godinho, M. H., & Fernando, A. L. (2022). Micro and nanocellulose extracted from energy crops as reinforcement agents in chitosan films. *Industrial Crops and Products, 186*, Article 115247. https://doi.org/10.1016/j.indcrop.2022.115247
Qazanfarzadeh, Z., Ganesan, A. R., Mariniello, L., Conterno, L., & Kumaravel, V. (2023). Valorization of brewer's spent grain for sustainable food packaging. *Journal of Cleaner Production, 385*, Article 135726. https://doi.org/10.1016/j.jclepro.2022.135726
Raza, M., Abu-Jdayil, B., Banat, F., & Al-Marzouqi, A. H. (2022). Isolation and characterization of cellulose nanocrystals from date palm waste. *ACS Omega, 7*, 25366–25379. https://doi.org/10.1021/acsomega.2c02333
Reddy, J. P., & Rhim, J. W. (2018). Extraction and characterization of cellulose microfibers from agricultural wastes of onion and garlic. *Journal of Natural Fibers, 15*, 465–473. https://doi.org/10.1080/15440478.2014.945227
Ren, H., Shen, J., Pei, J., Wang, Z., Peng, Z., Fu, S., & Zheng, Y. (2019). Characteristic microcrystalline cellulose extracted by combined acid and enzyme hydrolysis of sweet sorghum. *Cellulose, 26*, 8367–8381. https://doi.org/10.1007/s10570-019-02712-6
Restaino, O. F., Giosafatto, C. V. L., Mirpoor, S. F., Cammarota, M., Hejazi, S., Mariniello, L., Schiraldi, C., & Porta, R. (2023). Sustainable exploitation of *Posidonia oceanica* sea balls (egagropili): A review. *International Journal of Molecular Sciences, 24*, 7301. https://doi.org/10.3390/ijms24087301
Rovera, C., Carullo, D., Bellesia, T., Büyüktaş, D., Ghaani, M., Caneva, E., & Farris, S. (2023). Extraction of high-quality grade cellulose and cellulose nanocrystals from different lignocellulosic agri-food wastes. *Frontiers in Sustainable Food Systems, 6*, Article 1087867. https://doi.org/10.3389/fsufs.2022.1087867
Rovera, C., Ghaani, M., Santo, N., Trabattoni, S., Olsson, R. T., Romano, D., & Farris, S. (2018). Enzymatic hydrolysis in the green production of bacterial cellulose nanocrystals. *ACS Sustainable Chemistry & Engineering, 6*, 7725–7734. https://doi.org/10.1021/acssuschemeng.8b00600

Sejati, P. S., Akong, F. O., Torloting, C., Fradet, F., & Gérardin, P. (2022). Fully wood based novel translucent and thermoplastic materials by solvent-free esterification. *RSC Advances, 12*, 35206–35214. https://doi.org/10.1039/D2RA06555J

Shi, H., Wu, L., Luo, Y., Yu, F., & Li, H. (2022). A facile method to prepare cellulose fiber-based food packaging papers with improved mechanical strength, enhanced barrier, and antibacterial properties. *Food Bioscience, 48*, Article 101729. https://doi.org/10.1016/j.fbio.2022.101729

Suárez, L., Barczewski, M., Kosmela, P., Marrero, M. D., & Zaida, O. (2022). Giant reed (*Arundo donax* L.) fiber extraction and characterization for its use in polymer composites. *Journal of Natural Fibers, 20*, Article 2131687. https://doi.org/10.1080/15440478.2022.2131687

Tarchoun, A. F., Trache, D., & Klapötke, T. M. (2019). Microcrystalline cellulose from *Posidonia oceanica* brown algae: Extraction and characterization. *International Journal of Biological Macromolecules, 138*, 837–845. https://doi.org/10.1016/j.ijbiomac.2019.07.176

Thuy, V. T. T., Hao, L. T., Jeon, H., Koo, J. M., Park, J., Lee, E. S., Hwang, S. Y., Choi, S., Park, J., & Oh, D. X. (2021). Sustainable, self-cleaning, transparent, and moisture/oxygen-barrier coating films for food packaging. *RSC Green Chemistry, 23*, 2658. https://doi.org/10.1039/d0gc03647a

Vallejo, M., Cordeiro, R., Dias, P. A. N., Moura, C., Henriques, M., Seabra, I. J., Malça, C. M., & Morouço, P. (2021). Recovery and evaluation of cellulose from agroindustrial residues of corn, grape, pomegranate, strawberry-tree fruit and fava. *Bioresources and Bioprocessing, 8*, 25. https://doi.org/10.1186/s40643-021-00377-3

Vellingiri, V., Amendola, D., & Spigno, G. (2014). Screening of four different agro-food by-products for the recovery of antioxidants and cellulose. *Chemical Engineering Transactions, 37*, 757–762. https://doi.org/10.3303/CET1437127

Voca, N., Grubor, M., Peter, A., & Kricka, T. (2019). Evaluation of *Posidonia oceanica* waste as a biomass source for energy generation. *BioEnergy Research, 12*, 1104–1112. https://doi.org/10.1007/s12155-019-10032-7

Wang, L., Li, Y., Ye, L., Zhi, C., Zhang, T., & Miao, M. (2024). Pu-Erh tea-derived cellulose exhibits superior water/oil holding capacity compared to black and green tea celluloses: A comprehensive analysis. *Food Bioscience, 59*, Article 104073. https://doi.org/10.1016/j.fbio.2024.104073

Yogalakshmi, K. N., Mohamed Usman, T. M., Kavitha, S., Sachdeva, S., Thakur, S., Adish Jumar, S., & Rajesh Banu, J. (2023). Lignocellulosic biorefinery technologies: A perception into recent advances in biomass fractionation, biorefineries, economic hurdles and market outlook. *Fermentation, 9*, 238. https://doi.org/10.3390/fermentation9030238

Zeleke, N. M., Sinha, D. K., & Mengesha, G. A. (2022). Chemical composition and extraction of micro crystalline cellulose from outer skin isolated coffee husk. *Advances in Materials Science and Engineering*. https://doi.org/10.1155/2022/7163359